Figure 2. **Straight-Line Fits to Temperature Readings** of top- and bottom-plate thermocouples were used to calculate the supersaturation as a function of position along the width axis of the chamber.

- The main chamber is bounded on the top and bottom by parallel thick copper plates, which are joined by a thermally conductive vertical wall on one side and a thermally nonconductive wall on the opposite side.
- To establish a temperature gradient needed to establish a supersaturation gradient, water at two different regulated temperatures is pumped through tubes along the edges of the copper plates at the thermally-non-conductive-wall side. Figure 2 presents an example of temperature and supersaturation gradients for one combination of regulated tempera-

tures at the thermally-nonconductive-wall edges of the copper plates.
- To enable measurement of the temperature gradient, ten thermocouples are cemented to the external surfaces of the copper plates (five on the top plate and five on the bottom plate), spaced at equal intervals along the width axis of the main chamber near the outlet end.
- Pieces of filter paper or cotton felt are cemented onto the interior surfaces of the copper plates and, prior to each experimental run, are saturated with water to establish a supersaturation field inside the main chamber.

- A flow of monodisperse aerosol and a dilution flow of humid air are introduced into the main chamber at the inlet end. The inlet assembly is designed to offer improved (relative to prior such assemblies) laminar-flow performance within the main chamber. Dry aerosols are subjected to activation and growth in the supersaturation field.
- After aerosol activation, at the outlet end of the main chamber, a polished stainless-steel probe is used to sample droplets into a laser particle counter. The probe features an improved design for efficient sampling. The counter has six channels with size bins in the range of 0.5- to 5.0-μm diameter.
- To enable efficient sampling, the probe is scanned along the width axis of the main chamber (thereby effecting scanning along the temperature gradient and thereby, further, effecting scanning along the supersaturation gradient) by means of a computer-controlled translation stage.

This work was done by Ming-Taun Leu of Caltech for NASA's Jet Propulsion Laboratory.

# Better Modeling of Electrostatic Discharge in an Insulator

A model based on Kohlrausch relaxation gives improved fits to experimental data.

NASA's Jet Propulsion Laboratory, Pasadena, California

An improved mathematical model has been developed of the time dependence of buildup or decay of electric charge in a high-resistivity (nominally insulating) material. The model is intended primarily for use in extracting the DC electrical resistivity of such a material from voltage-vs.-current measurements performed repeatedly on a sample of the material over a time comparable to the longest characteristic times (typically of the order of months) that govern the evolution of relevant properties of the material. This model is an alternative to a prior simplistic macroscopic model that yields results

differing from the results of the time-dependent measurements by two to three orders of magnitude.

The present model is based on the Kohlrausch relaxation law, named after its author, who first reported a long-lasting dielectric relaxation in 1854. Since then, the Kohlrausch law has been used to describe a myriad of physical phenomena. Kohlrausch relaxation is also known as stretched exponential relaxation because the time-dependent value of a Kohlrausch-relaxing quantity of interest is proportional to the stretched exponential function $\exp[(-t/\tau)^{\beta}]$
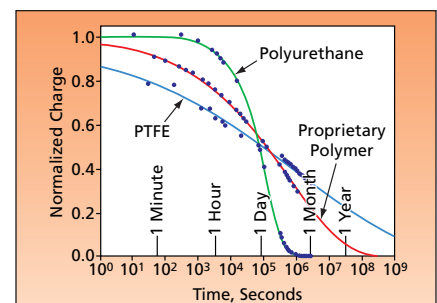
Kohlrausch Fits (the solid curves) were made to normalized-charge data calculated from long-term measurements on three different dielectrics: a poly(tetrafluoroethylene) [PTFE], a polyurethane, and a proprietary polymer.

where t is time, τ is a characteristic relaxation time of the material in question, and β is a parameter (sometimes denoted the Kohlrausch exponent) that has a value between 0 and 1. Many microscopic models of transport in distributed systems (e.g., electron hopping, dipole fluctuation) have shown to result in Kohlrausch dependences of macroscopic observables.

In general, whichever model is used, the DC electrical resistivity of a material sample subjected to long-term charge-decay measurements is calculated from parameters used to fit the model to the measurement data. Various methods that have been used to fit simplistic macroscopic models to measurement data involve large numbers of fitting parameters and involve user-dependent fitting calculations. In contrast, the Kohlrausch-relaxation-based model involves the minimum possible number of fitting parameters, and the associated fitting calculations are not user-dependent.

The applicability of the present model and its superiority to the prior macroscopic model have been demonstrated through the closeness with which this model has been shown to fit experimental data on normalized charge over 5 to 6 orders of magnitude in time (for example, see figure). Although the validity of DC-resistivity values derived from fitting parameters of this model has yet to be demonstrated, the mere fact that these resistivity values differ from those obtained by application of the prior macroscopic model to the same experimental data indicates the need for further research to answer the questions of what are the relevant properties of the affected materials and what are the proper methods of determining these properties.

Sub-Aperture Interferometers

## Multiple target sub-beams are derived from the same measurement beam.

NASA's Jet Propulsion Laboratory, Pasadena, California

Sub-aperture interferometers — also called wavefront-split interferometers — have been developed for simultaneously measuring displacements of multiple targets. The terms "sub-aperture" and "wavefront-split" signify that the original measurement light beam in an interferometer is split into multiple sub-beams derived from non-overlapping portions of the original measurement-beam aperture. Each measurement sub-beam is aimed at a retroreflector mounted on one of the targets. The splitting of the measurement beam is accomplished by use of truncated mirrors and masks, as shown in the example below.

Sub-aperture interferometers incorporate some of the innovations described in two previous *NASA Tech Briefs* articles: "Common-Path Heter-
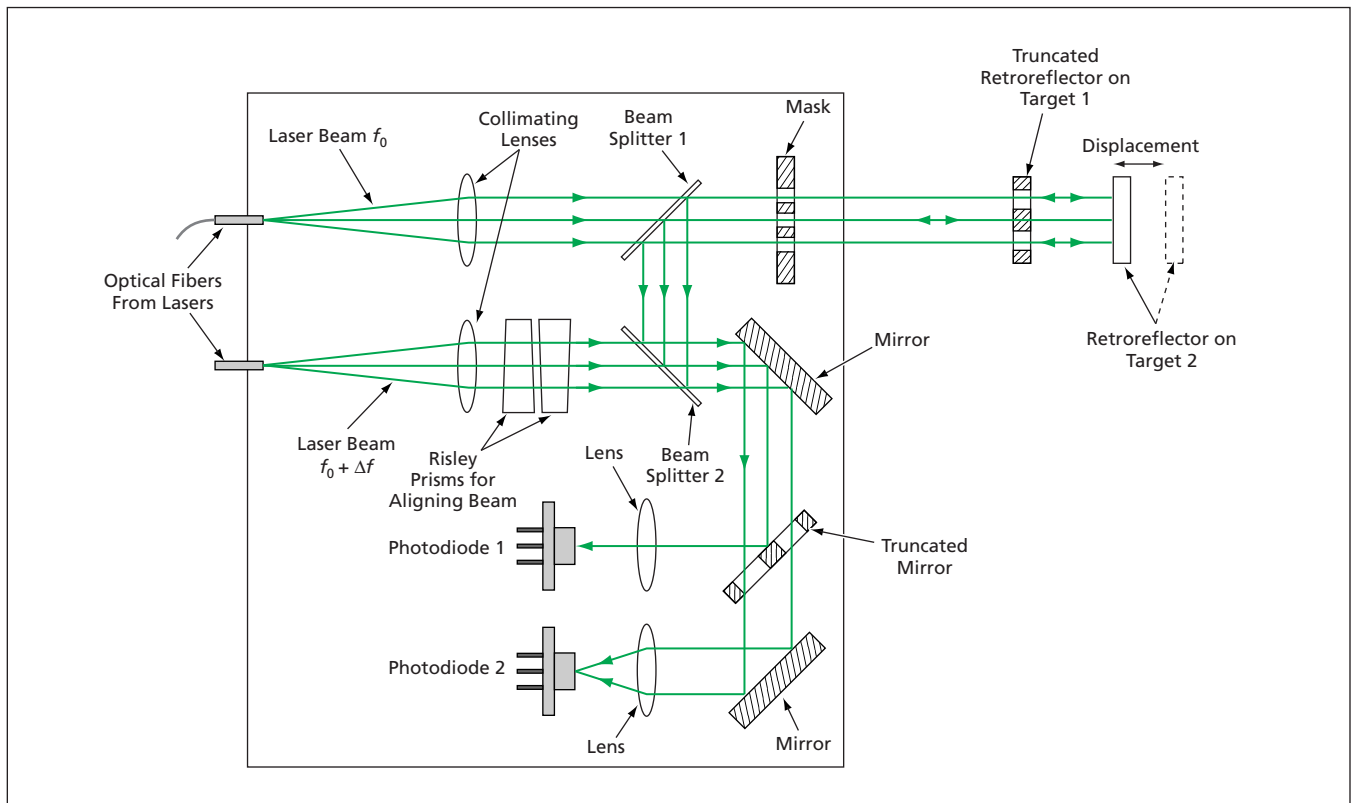
In this **Wavefront-Split Interferometer**, the truncated retroreflector on the first target and the retroreflector on the second target form a measurement optical cavity. The roles played by the measurement and reference beams in a typical prior interferometer are here played by two measurement sub-beams derived from the same measurement beam without use of extra optics.